Supporting Information Figures for 'Evaluation of Principal Component Analysis Image Denoising on Multi-Exponential MRI Relaxometry', by Does, Olesen, Harkins, Serradas-Duarte, Gochberg, Jespersen, and Shemesh.

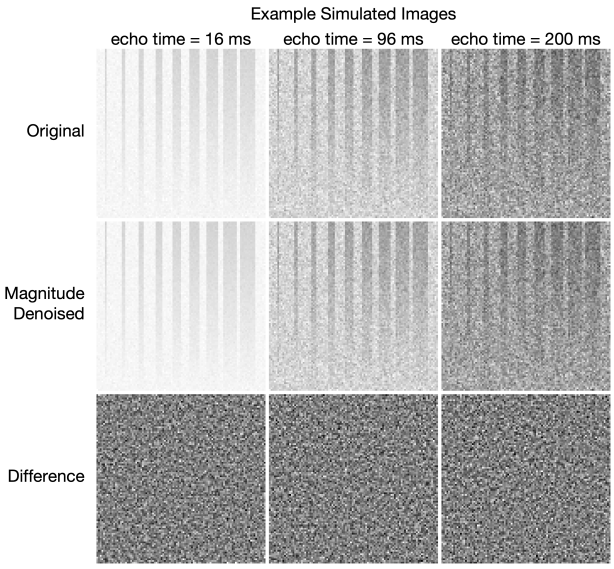

Figure S1: Example simulated images from the scenario with $N_{\mathrm{E}} = 40$, $T_{\mathrm{E}} = 8\,\mathrm{ms}$, $\sigma_{\mathrm{T2l}} = 5\,\mathrm{ms}$, and $\mathrm{SNR} = 200$. The top row shows original noisy images. The second and third rows show the magnitude denoised images and the difference images, respectively. At each different echo time, the original and denoised images are all displayed using the same grayscale, and all three differences images are scaled to $\pm 3\sigma$.

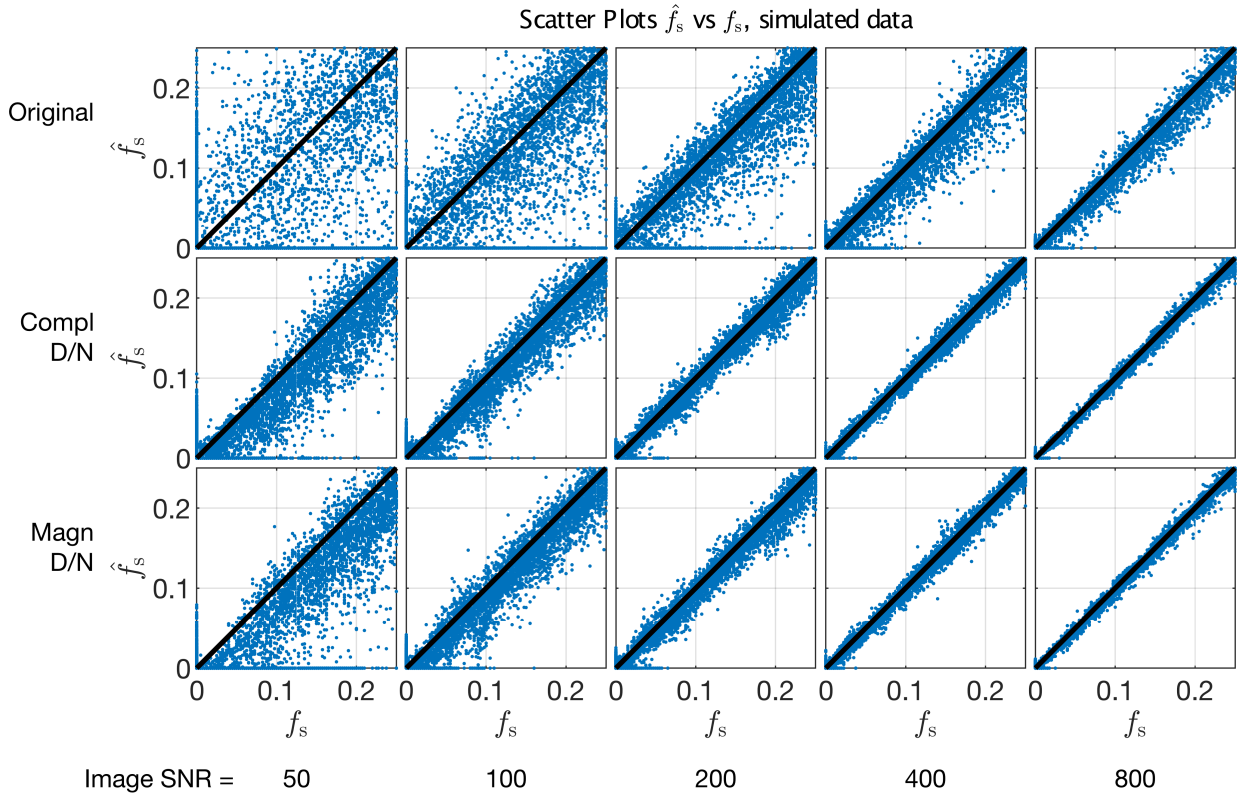

Figure S2: Scatter plots of estimate short T_2 signal fraction, $\hat{f}_s$, vs the ground truth, f_s, for the example scenario of $N_E = 40$, $T_E = 8\,\text{ms}$, and $\sigma_{T2l} = 5\,\text{ms}$.

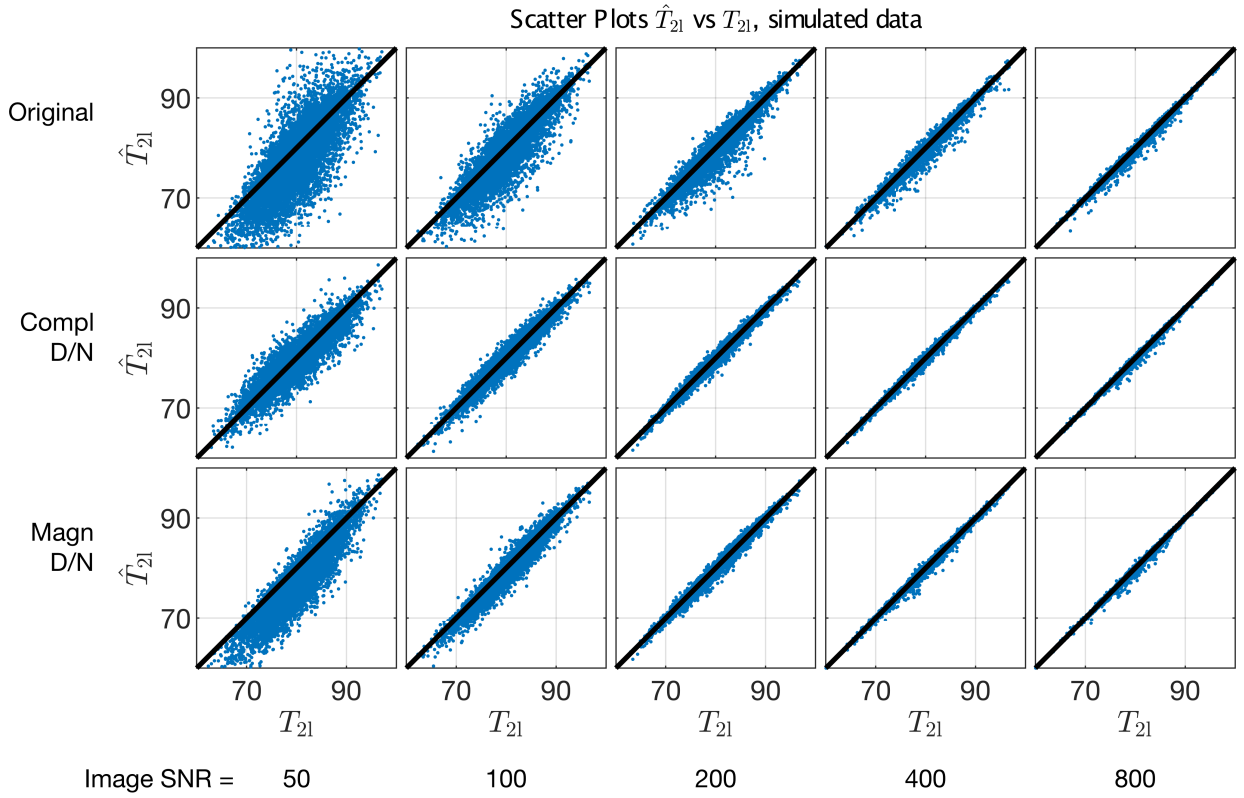

Figure S3: Scatter plots of estimate long T_2, $\hat{T}_{2l}$, vs the ground truth, T_{2l}, for the example scenario of $N_E = 40$, $T_E = 8\,\text{ms}$, and $\sigma_{T2l} = 5\,\text{ms}$.

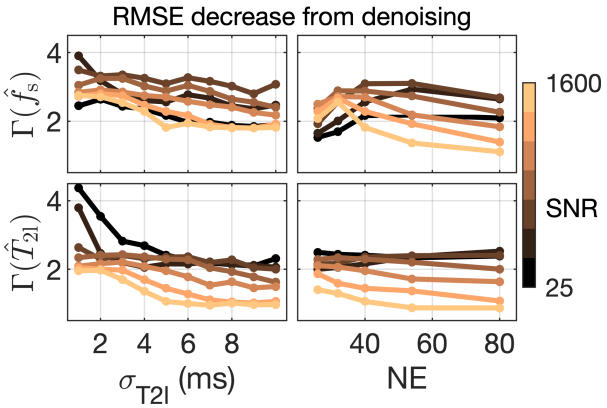

Figure S4: Measure of the relative decrease in parameter RMSE due to denoising, as a function of σ_{T2l} (left), N_E (right), and image SNR (color). For all frames, the vertical axis is $\Gamma(p) \triangleq \text{RMSE}_o(p)/\text{RMSE}_d(p)$, where subscripts 'o' and 'd' indicate 'original' and 'denoised', respectively, and 'p' is the fitted parameter of interest.

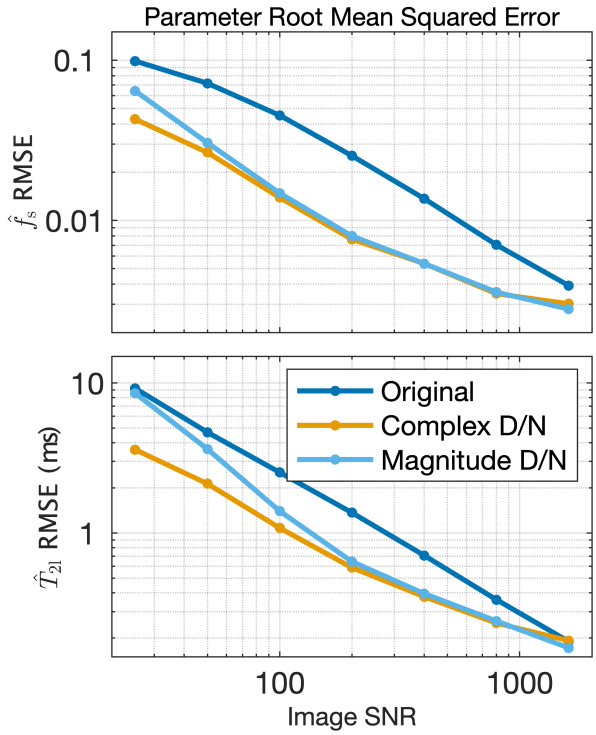

Figure S5: RMSE values of $\hat{f}_s$ and $\hat{T}_{2l}$ computed from original and denoised images, for simulations using $\theta = 155°$ and image SNR values 50 to 1600.

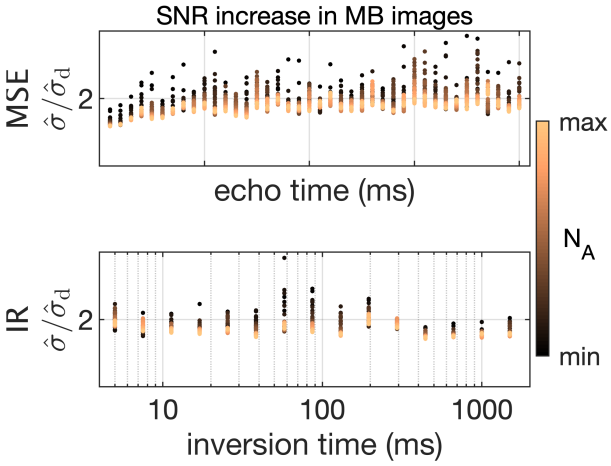

Figure S6: Relative increase in mouse brain image SNR after denoising, as a function of echo time (MSE, top) or inversion time (IR, bottom) and N_A (color). Note that N_A ranges 4 to 256 for MSE and 1 to 64 for IR.

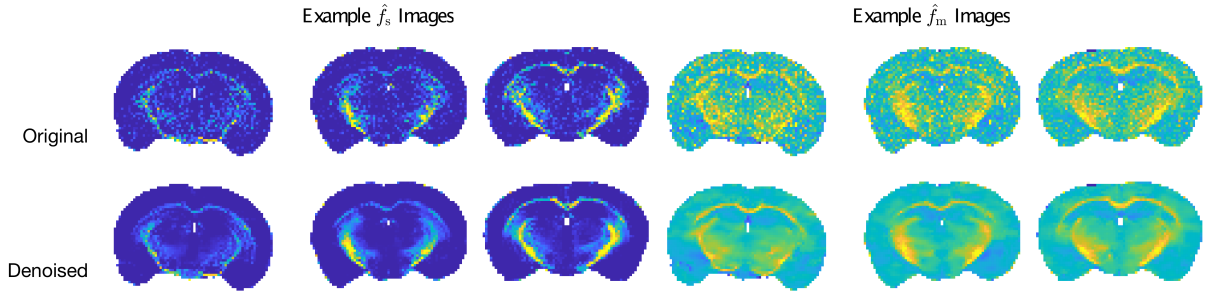

Figure S7: Example $\hat{f}_s$ and $\hat{f}_m$ parameter maps from three different mouse brains. Parameter intensities vary some between brains/slice location, but the improvement in parameter map quality due to denoising is qualitatively similar in all cases.

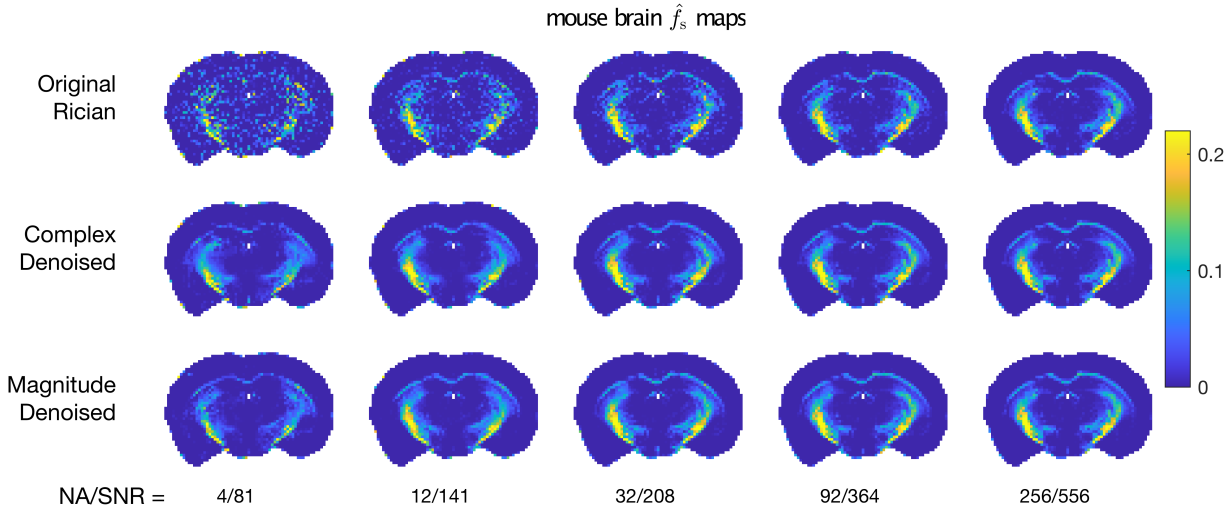

Figure S8: A comparison of $\hat{f}_s$ maps from original, complex denoised, and magnitude denoised images. Except at low image SNR, the effect of complex and magnitude denoising on $\hat{f}_s$ maps was similar.

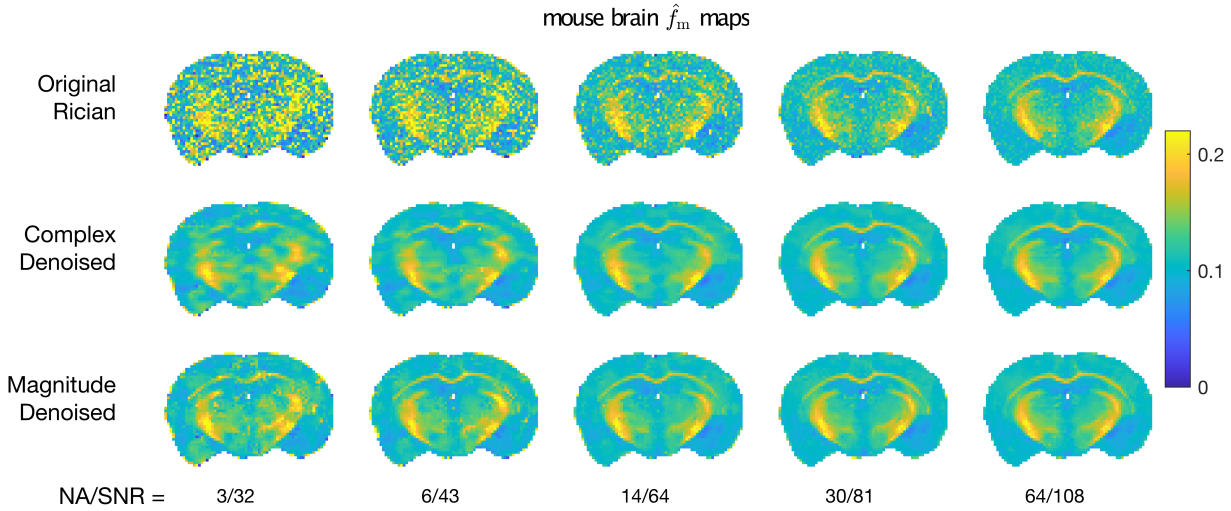

Figure S9: A comparison of $\hat{f}_{\mathrm{m}}$ maps from original, complex denoised, and magnitude denoised images. Except at low image SNR, the effect of complex and magnitude denoising on $\hat{f}_{\mathrm{m}}$ maps was similar.

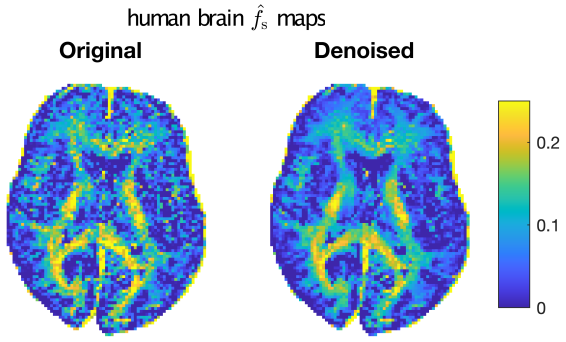

Figure S10: A comparison of $\hat{f}_{\mathrm{s}}$ maps from original and magnitude denoised images acquired with an 8-channel receive coil on a Philips 3.0T scanner. The PCA denoising was done by retaining a fixed $P = 4$ principal components, rather than using the MP algorithm.